Table I. Spectroscopic Parameters for Uracil[a]

A	3883878.25 (110)	D_K	0.4724 (43)
B	2023732.67 (101)	d_1	-0.02738 (28)
C	1330923.80 (60)	d_2	-0.006532 (94)
D_J	0.06029 (77)	Δ	-0.128 uÅ^2
D_{JK}	0.1047 (14)		

[a] In kHz except for Δ.

Furthermore, the rotational constants agree to within better than 1% with those expected for the diketo tautomer. We have not detected any strong lines that could be assigned to other tautomeric forms, implying that the diketo form is the most stable tautomer in the gas phase. This is in agreement with various theoretical studies of the relative stabilities of the tautomers,[8] the tautomer observed in the crystal[5,6] and that which is inferred as the major gas-phase tautomer from the fluorescence studies,[4] although in the latter a small fraction of a keto-enol tautomer was thought to exist.

We have been able to observe only relatively high-J lines for which precise Stark effect measurements are not feasible. However it has been possible to make limited observations of the Stark effect for the $18_{6,13}$-$17_{6,12}$ and $18_{4,14}$-$17_{5,13}$ lines from which we derive dipole moment components of $\mu_a = 1.61$ D and $\mu_b = 3.52$ D; hence, $\mu = 3.87$ D (errors are estimated to be less than 10%). Our value for the total moment is close to the value (4.16 D) measured in dioxane solution.[9]

Further work is planned on other isotopic versions of uracil in order to derive more complete structural information.

Supplementary Material Available: A table of observed and calculated transition frequencies used to derive the data in Table I (4 pages). Ordering information is given on any current masthead page.

(8) Scanlan, M. J.; Hillier, I. H. *J. Am. Chem. Soc.* **1984**, *106*, 3737-3745. Les, A.; Ortega-Blake, I. *Int. J. Quantum Chem.* **1986**, *30*, 225-237.
(9) Kulakowski, I.; Geller, M.; Lesyng, B.; Weirzchowski, K. L. *Biochim. Biophys. Acta* **1974**, *361*, 119-130.

Structural Characterization by EXAFS Spectroscopy of the Binuclear Iron Center in Protein A of Methane Monooxygenase from *Methylococcus capsulatus* (Bath)

Agneta Ericson, Britt Hedman, and Keith O. Hodgson*

Stanford Synchrotron Radiation Laboratory and Department of Chemistry, Stanford University Stanford, California 94305

Jeffrey Green and Howard Dalton*

Department of Biological Sciences, University of Warwick, Coventry, CV4 7AL, United Kingdom

James G. Bentsen, Robert H. Beer, and Stephen J. Lippard*

Department of Chemistry Massachusetts Institute of Technology Cambridge, Massachusetts 02139

Received September 14, 1987

Soluble methane monooxygenase (MMO) from *Methylococcus capsulatus* (Bath)[1-3] activates dioxygen for incorporation into a remarkable variety of substrates[2] including methane, which is required for bacterial growth (eq 1). MMO is a three-component

$$CH_4 + NADH + H^+ + O_2 \xrightarrow{MMO} CH_3OH + NAD^+ + H_2O \quad (1)$$

enzyme. Protein A (M_r 210000), believed to be the oxygenase component, contains two iron atoms per molecule of protein.[4] Protein B (M_r 15700) serves a regulatory function and lacks prosthetic groups,[5] while protein C, the reductase component of the enzyme, is an iron-sulfur flavoprotein (M_r 42000) responsible for electron transfer from NADH to protein A.[6] Recently, a binuclear iron center was postulated[7] to occur in protein A based on the finding that one-electron reduction gives rise to electron spin resonance (ESR) signals (g 1.95, 1.88, 1.78) very similar to those observed for the binuclear mixed-valence Fe_2(III,II) centers in semimet hemerythrin (Hr)[8] and purple acid phosphatase (PAP).[9] In conjunction with model studies, extended X-ray absorption fine structure (EXAFS) spectroscopy has proved to be a powerful method for identifying bridged binuclear iron centers in Hr,[10,11a] ribonucleotide reductase (RR),[11] and PAP.[12] Here we report iron K-edge EXAFS results on semireduced protein A of MMO which support the occurrence of a binuclear iron center (Fe-Fe distance, 3.41 Å), with no short μ-oxo bridge.

Purified protein A of *M. capsulatus* (Bath) MMO[4] was dissolved in 25 mM pH 7.0 Pipes buffer, concentrated, diluted with glycerol to a final concentration of 10% glycerol, frozen in liquid nitrogen, and stored at -80 °C. The final protein concentration was ~385 mg/mL, and the iron content was determined by flameless atomic absorption spectroscopy to be 2.1 ± 0.1 mol Fe (3.8 mM Fe) per mol protein. X-ray absorption data were collected at the Stanford Synchrotron Radiation Laboratory on the focused beam line II-2 under dedicated conditions (3.0 GeV, 50-65 mA) by using a Si(111) double-crystal monochromator. All protein data were measured at 10 K as Mn filtered fluorescence excitation spectra monitored by an argon-filled ionization chamber.[13] Data reduction and analysis were performed as previously reported.[14,15] Curve-fitting techniques were applied by using empirical phase and amplitude parameters for various Fe-X scattering pairs obtained from the following models: Fe-O and Fe-C, [Fe(acetylacetonate)$_3$];[16] Fe-N, [Fe(1,10-phenanthroline)$_3$](ClO$_4$)$_2$;[17] Fe-Fe, [Fe$_2$(OH)(OAc)$_2$(HBpz$_3$)$_2$](ClO$_4$) (**1**).[18] Data were also collected for [Fe$_2$O-

(1) Colby, J.; Dalton, H. *Biochem. J.* **1976**, *157*, 495-497.
(2) Colby, J.; Stirling, D. I.; Dalton, H. *Biochem. J.* **1977**, *165*, 395-402.
(3) Colby, J.; Dalton, H. *Biochem. J.* **1978**, *171*, 461-468.
(4) (a) Woodland, M. P.; Dalton, H. *J. Biol. Chem.* **1984**, *259*, 53-59. (b) Woodland, M. P.; Dalton, H. *Anal. Biochem.* **1984**, *139*, 459-462.
(5) Green, J.; Dalton, H. *J. Biol. Chem.* **1985**, *260*, 15795-15801.
(6) Lund, J.; Woodland, M. P.; Dalton, H. *Eur. J. Biochem.* **1985**, *147*, 297-305.
(7) Woodland, M. P.; Patil, D. S.; Cammack, R.; Dalton, H. *Biochim. Biophys. Acta* **1986**, *873*, 237-242.
(8) (a) Wilkins, R. G.; Harrington, P. C. *Adv. Inorg. Biochem.* **1983**, *5*, 51-85. (b) Harrington, P. C.; Wilkins, R. G. *Coord. Chem. Rev.* **1987**, *7*, 195-214.
(9) Antanaitis, B. C.; Aisen, P. *Adv. Inorg. Biochem.* **1983**, *5*, 111-136.
(10) (a) Hendrickson, W. A.; Co, M. S.; Smith, J. L.; Hodgson, K. O.; Klippenstein, G. L. *Proc. Natl. Acad. Sci. U.S.A.* **1982**, *79*, 6255-6259. (b) Elam, W. T.; Stern, E. A.; McCallum, J. D.; Sanders-Loehr, J. *J. Am. Chem. Soc.* **1983**, *105*, 1919-1923. (c) Hedman, B.; Co, M. S.; Armstrong, W. H.; Hodgson, K. O.; Lippard, S. J. *Inorg. Chem.* **1986**, *25*, 3708-3711.
(11) (a) Scarrow, R. C.; Maroney, M. J.; Palmer, S. M.; Que, L., Jr.; Roe, A. L.; Salowe, S. P.; Stubbe, J. *J. Am. Chem. Soc.* **1987**, *109*, 7857-7864. (b) Scarrow, R. C.; Maroney, M. J.; Palmer, S. M.; Que, L., Jr.; Salowe, S. P.; Stubbe, J. *J. Am. Chem. Soc.* **1986**, *108*, 6832-6834. (c) Bunker, G.; Peterson, L.; Sjöberg, B.-M.; Sahlin, M.; Chance, M.; Chance, B.; Ehrenberg, A. *Biochemistry* **1987**, *26*, 4708-4716.
(12) Kauzlarich, S. M.; Teo, B. K.; Zirino, T.; Burman, S.; Davis, J. C.; Averill, B. A. *Inorg. Chem.* **1986**, *25*, 2781-2785.
(13) (a) Lytle, F. W.; Greegor, R. B.; Sandstrom, D. R.; Marques, E. C.; Wong, J.; Spiro, C. L.; Huffman, G. P.; Huggins, F. E. *Nucl. Instr. Meth.* **1984**, *226*, 542-548. (b) Stern, E. A.; Heald, S. M. *Rev. Sci. Instr.* **1979**, *50*, 1579-1582.
(14) Energy calibration was performed by using the internal standard method (Scott, R. A.; Hahn, J. E.; Doniach, S.; Freeman, H. C.; Hodgson, K. O. *J. Am. Chem. Soc.* **1982**, *104*, 5364-5369), assigning the first inflection point of the Fe K absorption edge for Fe foil as 7111.2 eV. The normalized background-subtracted data were converted to k-space by assuming a threshold energy (E_0) of 7130 eV. The photoelectron wave vector k is defined by $k = (2m_e(E - E_0)/\hbar^2)^{1/2}$, where m_e is the electron mass.
(15) (a) Eccles, T. K. Ph.D. Dissertation, Stanford University, 1977. (b) Cramer, S. P.; Hodgson, K. O. *Prog. Inorg. Chem.* **1979**, *15*, 1-39. (c) Scott, R. A. *Meth. Enzymol.* **1985**, *117*, 414-459.
(16) (a) Roof, R. B. *Acta Crystallogr.* **1956**, *9*, 781-786. (b) Iball, J.; Morgan, C. H. *Acta Crystallogr.* **1967**, *23*, 239-244.
(17) Synthesized according to Johansson (Johansson, L. *Chem. Scr.* **1976**, *9*, 30-35). The crystal structure of the perchlorate salt has not been determined, but the [Fe(phenanthroline)$_3$]$^{2+}$ complex structure can be assumed to be identical with that of the corresponding iodide salt. The synthesis of the latter was reported in the same paper, and the crystal structure determination by Johansson et al. (Johansson, L.; Molund, M.; Oskarsson, Å. *Inorg. Chim. Acta* **1978**, *31*, 117-123).

0002-7863/88/1510-2330$01.50/0

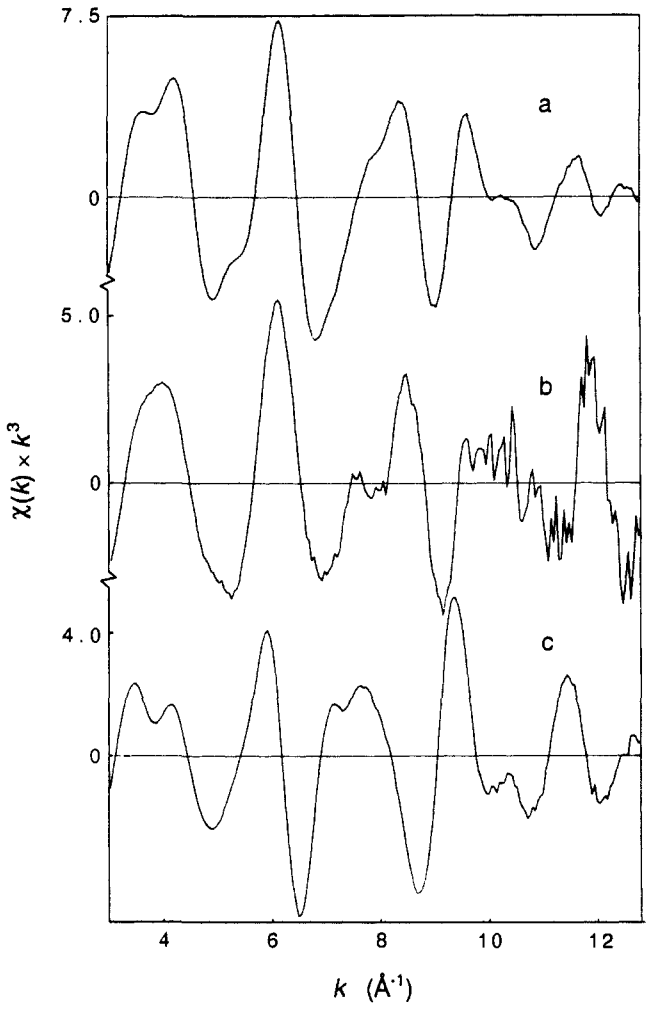

Figure 1. EXAFS multiplied by k^3 of (a) $[Fe_2(OH)(OAc)_2(HBpz_3)_2](ClO_4)$ (**1**); (b) protein A of MMO; and (c) $[Fe_2O(OAc)_2(HBpz_3)_2]$ (**2**). Note the striking correspondence between the protein A and the (μ-hydroxo)diiron(III) complex, relative to the dissimilarity for protein A and the (μ-oxo)diiron(III) complex.

$(OAc)_2(HBpz_3)_2]$ (**2**).[19] All models were measured in the transmission mode under the same conditions as the protein, except for the phenanthroline complex, where the unfocused wiggler beam line VII-3 and a Si(220) monochromator were used.

The edge position of the protein spectrum shifted gradually by ~1.5 eV to lower energy over the first seven scans, after which it remained constant. This shift is most likely an effect of photoreduction of the iron center by the X-ray beam. Additional experiments[20] establish that a comparable edge-shift accompanies one-electron X-ray induced photoreduction to give an ESR-detected mixed-valence Fe_2(III,II) species (g 1.92, 1.85, 1.72) in high yield. Only the later scans, where the edge position was constant (scans 8–32), were averaged and used in the final curve-fitting analyses for which the results are reported herein. The only distinguishable difference in the EXAFS data between an average of the early scans (1–7) and the energy-consistent later scans was a slightly lower amplitude for the latter, which resulted in lower coordination numbers (~10%) when results from fits were compared.

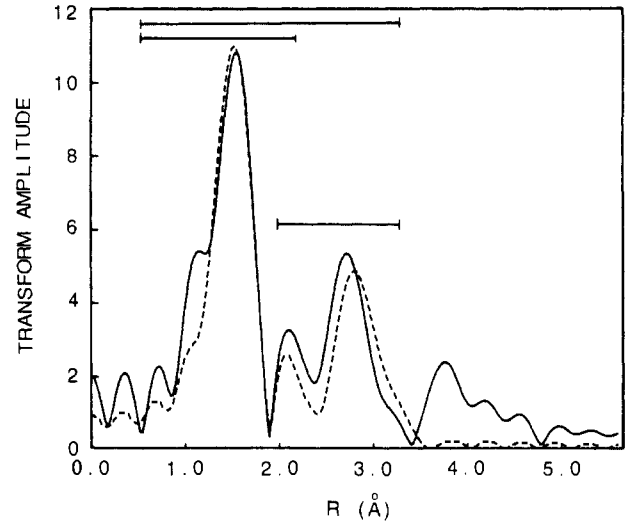

Figure 2. Fourier transform of experimental data for protein A of MMO over the k range 3.5–12.2 Å^{-1} (solid line). The horizontal bars indicate the width of the windows used for back-transforming (filtering) the data for (top to bottom) two-shell, first-shell, and second-shell curve fits. Numerical information is given in Table I. The Fourier transform of the calculated EXAFS from the fit shown in Figure 3 is included for comparison (dashed line).

Table I. EXAFS Curve-Fitting Results for Methane Monooxygenase, Protein A[a,d]

	Fe–N[b]		Fe–O[b]		Fe–Fe		Fe–C		
filter	R, Å	n[c]	R, Å	n[c]	R, Å	n[c]	R, Å	n[c]	F
1	2.02	3.1							0.80
1	2.20	1.9	1.99	3.4					0.42
2					3.41	0.8			0.45
3	2.20	2.0	1.99	3.5	3.41	0.8			0.54
3	2.20	2.0	1.99	3.5	3.42	1.0	3.27	2.6	0.51

[a] EXAFS fitting range k = 3.5–12.2 Å^{-1}. Errors are estimated to be about ±0.03 Å for distances and 25% for coordination numbers.[15b,23] [b] An equally good fit is obtained if the Fe–O/Fe–N assignments are reversed in the fits, resulting in 4.0 N at 2.00 Å and 1.7 O at 2.13 Å. [c] The number (n) of ligands at the distance (R), the only parameters varied in the refinements. [d] The three different filters used for these fits were as follows: (1) 0.52–2.20 Å; (2) 2.00–3.33 Å; (3) 0.52–3.33 Å. A Gaussian window of 0.1 Å was used for all filters.

The EXAFS (multiplied by k^3) spectra for the (μ-hydroxo)diiron(III) complex (**1**), protein A of MMO, and the (μ-oxo)diiron(III) complex (**2**) are compared in Figure 1. There is a close correspondence in the EXAFS for protein A and the (μ-hydroxo)diiron(III) complex, particularly in the frequency, which indicates that iron in protein A has metrical details similar to that of the μ-hydroxo binuclear center. There is very little resemblance in the EXAFS of protein A and the (μ-oxo)diiron(III) complex. The Fourier transform of the EXAFS data of protein A is shown in Figure 2. Curve-fitting was performed on filtered first- and second-shell contributions as well as for a two-shell filter, as indicated in Figure 2. The resulting bond distances and coordination numbers are listed in Table I. The first-shell data could not be adequately fit with a single shell of N or O. Including separate waves for N and O greatly improved the fit, and the function value, F, decreased significantly from 0.80 to 0.42.[21] The

(18) Armstrong, W. H.; Lippard, S. J. *J. Am. Chem. Soc.* **1984**, *106*, 4632–4633.

(19) Armstrong, W. H.; Spool, A.; Papaefthymiou, G. C.; Frankel, R. B.; Lippard, S. J. *J. Am. Chem. Soc.* **1984**, *106*, 3653–3667.

(20) X-ray absorption measurements for protein A (in the initial oxidized state) have recently been repeated in degassed 20 mM sodium phosphate buffer (50% ethylene glycol, pH 7.0). Data have also been collected for the two-electron reduced form of protein A (the results of these studies will be reported later). A comparable edge-shift of about 1.7 eV to lower energy was seen when the oxidized sample was recollected over a similar irradiation time. In contrast, the reduced sample showed no detectable change in edge position. The energy difference between the first scan of the oxidized sample and any of the scans of the reduced sample was about 4 eV. A summation of the first edge of the oxidized sample with a scan of the reduced sample results in an edge that is similar to that observed for edges of the samples that were averaged to give the data used in the analysis reported in this communication (scans 8–31). ESR spectra for the photoreduced sample were obtained at 4–30 K and indicated the presence of a free radical (g = 2.0) and a photogenerated Fe_2(III,II) species (g 1.92, 1.85, 1.72). Warmup to 298 K, followed by recooling to 4 K, resulted in loss of only the g = 2 signal. Subsequent integration versus a Cu–EDTA standard indicated > 70% ± 20% net conversion of oxidized protein A to the mixed-valence state.

(21) The function value, F, is defined as $\{\sum[k^6(\text{data-fit})^2]/(\text{no. of points})\}^{1/2}$.

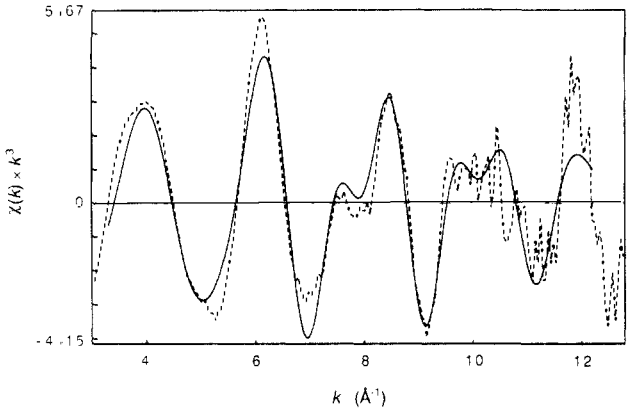

Figure 3. Comparison of the least-squares fit (dark line) to the EXAFS data of protein A of MMO (dashed line). Three waves (O, N, Fe) were used to fit data over a range of k = 3.5 - 12.2 Å^{-1}. The filter window for the back transform was R = 0.52 - 3.33 Å.

first coordination shell is thus composed of approximately six nearest N/O neighbors at an average distance of ~2.05 Å. A short Fe–O distance could not be fit to the data at any stage of the refinements and consistently gave negative coordination numbers. We have previously shown the high sensitivity of EXAFS to the presence or absence of a short μ-oxo bridge in binuclear iron centers.[10c]

The second-shell and two-shell curve-fittings showed a remarkable consistency in indicating the presence of a pair of iron atoms. Irrespective of the initial values of Fe–N, Fe–O, and Fe–Fe bond distances, the fits gave an Fe–Fe distance of 3.41 Å and a coordination number of 0.8. Carbon atoms are most probably present at distances around 3.0–3.3 Å from the iron atoms. In second-shell and two-shell fits which included an Fe–C wave, an insignificant improvement in F of 7% and 6%, respectively, occurred when adding an Fe–C wave (Table I). Replacing the Fe–Fe wave by only an Fe–C wave did, however, not give an acceptable fit. A comparison of the data and the best fit including O, N, and Fe backscattering waves is given in Figure 3 and a comparison of corresponding Fourier transforms in Figure 2.

Tests were further made to ensure that the Fe–Fe distance was not biased due to the fact that the backscattering parameters were extracted from the μ-hydroxo model. The μ-oxo model data were thus fitted by using these Fe–Fe backscattering parameters, and this fit gave the correct distance of 3.16 Å. Extracting Fe–Fe backscattering parameters from the μ-oxo model data and applying them in fits on the μ-hydroxo model data as well as the protein A data gave the expected long distance in the model compound and further confirmed the previously derived protein results.

We can therefore conclude that protein A of MMO in its semireduced form has a binuclear iron center with an Fe–Fe distance of 3.41 Å and no short μ-oxo bridge.[22]

Acknowledgment. This work was supported by grants from the National Science Foundation (CHE 85-12129 to K.O.H.), the Gas Research Institute (5086-260-1209 to H.D.), and the National Institute of General Medical Sciences (GM 32134 to S.J.L.). The EXAFS experiments were performed at Stanford Synchrotron Radiation Laboratory, which is supported by the Department of Energy, Office of Basic Energy Sciences, and the National Institutes of Health, Biotechnology Resource Program, Division of Research Resources. A.E. is a visiting graduate student supported in part by the Department of Inorganic Chemistry, Lund University, Sweden. J.G.B. acknowledges support under NCI Training Grant CA 09112 and as an American Cancer Society Postdoctoral Fellowship award recipient.

Registry No. 1, 90886-32-1; 2, 86177-70-0; Fe, 7439-89-6; methane monooxygenase, 51961-97-8; [Fe(1,10-phenanthroline)$_3$](ClO$_4$)$_2$, 14586-54-0.

(22) These results suggest a similarity with the binuclear iron center in semimethemerythrin azide, which has an Fe–Fe distance of 3.46 Å.[11a] The Fe–Fe distance is different from that of 3.05 Å being reported for oxidized protein A from *Methylobacterium* CRL-26 (Prince, R. C.; George, G. N.; Savas, J. C.; Cramer, S. P.; Patel, R. N. *Biochim. Biophys. Acta* **1988**, *952*, 220–229).

(23) Cramer, S. P.; Hodgson, K. O.; Stiefel, E. I.; Newton, W. E. *J. Am. Chem. Soc.* **1978**, *100*, 2748–2761.

Synthesis and Structure of [CpRu(PPh$_3$)$_2$(SC$_2$H$_4$)]OSO$_2$CF$_3$. A Transition-Metal Analogue of an Episulfonium Salt

Jayantha Amarasekera, Thomas B. Rauchfuss,* and Scott R. Wilson

School of Chemical Sciences, University of Illinois at Urbana-Champaign Urbana, Illinois 61801

Received October 30, 1987

Recent studies in this laboratory and elsewhere have demonstrated the broad applicability of CpRu(PPh$_3$)$_n$ derivatives in probing metal–sulfur interactions.[1-6] The CpRu(PPh$_3$)$_2^+$ fragment is an unusually soft electrophile; as we indicated in a recent paper,[4] CpRu(PPh$_3$)$_2^+$ is a close relative to Ru(NH$_3$)$_5^{2+}$ which has so fruitfully been studied by Taube and co-workers.[7] This report describes an innovation in CpRu(PPh$_3$)$_2$X chemistry which appears to be generally useful and which we have employed in the synthesis of a stable metal complex of the simplest sulfur heterocycle, thiirane (ethylene sulfide).

Thiirane is often used in transition-metal chemistry as a source of sulfur atoms,[8] and we were interested in using it to generate [CpRu(PPh$_3$)$_2$S]$^+$.[4] In order to facilitate the expected sulfur atom transfer reaction we preactivated the ruthenium center by preparing CpRu(PPh$_3$)$_2$OTf (**1**, OTf is OSO$_2$CF$_3$).[9,10] Compound **1** was synthesized by the straightforward reaction of CpRu(PPh$_3$)$_2$Cl and AgOTf in dichloromethane solution. After removal of the AgCl, the pale yellow complex was precipitated with hexanes. Recrystallization from dichloromethane–hexane gave a 75% yield of **1**. Compound **1** is soluble in aromatic and chlorinated organic solvents and is stable toward traces of water. The triflate complex is a versatile reactant. For example, it forms well-behaved derivatives with a variety of Lewis bases, hydrogen, olefins, and all of the chalcogens.

(1) Draganjac, M. E.; Ruffing, C. J.; Rauchfuss, T. B. *Organometallics* **1985**, *4*, 1909.
(2) Howard, K. E.; Rauchfuss, T. B.; Rheingold, A. L. *J. Am. Chem. Soc.* **1986**, *108*, 297.
(3) Amarasekera, J.; Rauchfuss, T. B.; Rheingold, A. L. *Inorg. Chem.* **1987**, *26*, 2017.
(4) Amarasekera, J.; Rauchfuss, T. B.; Wilson, S. R. *Inorg. Chem.* **1987**, *26*, 3328.
(5) Sauer, N. N.; Angelici, R. J. *Organometallics* **1987**, *6*, 1146, and references therein.
(6) Bryndza, H. E.; Fong, L. L.; Paciello, R. A.; Tam, W.; Bercaw, J. E. *J. Am. Chem. Soc.* **1987**, *109*, 1444.
(7) Kuehn, C. G.; Isied, S. S. *Prog. Inorg. Chem.* **1980**, *27*, 153. Taube, H. *Survey Prog. Chem.* **1973**, *6*, 1.
(8) For an review of the early work on heavy metal derivatives of thiirane, see: Sander, M. *Chem. Rev.* **1966**, *66*, 297. Schunn, R. A.; Fritchie, C. J.; Prewitt, C. T. *Inorg. Chem.* **1966**, *5*, 892. Brûlet, C. R.; Isied, S. S.; Taube, H. *J. Am. Chem. Soc.* **1973**, *95*, 4758. Vergamini, P. J.; Kubas, G. J. *Prog. Inorg. Chem.* **1975**, *17*, 261. Balch, A. L. *Adv. Chem. Ser.* **1982**, *196*, 243. Xiao-zeng, Y.; Zhong-he, Z.; Jin-shun, H.; Fenske, R. F.; Dahl, L. F. In *New Frontiers in Organometallic and Inorganic Chemistry*; Yaozeng, H.; Yamamoto, A.; Teo, B.-K., Eds.; S. P. Richards: New Providence, NJ, 1984; p 257. Morrow, J. R.; Tonker, T. L.; Templeton, J. L. *Organometallics* **1985**, *4*, 745. Lorenz, I.-P.; Messelauser, J.; Hiller, W.; Conrad, M. *J. Organomet. Chem.* **1986**, *316*, 121. Calet, S.; Alper, H. *Tetrahedron Lett.* **1986**, *27*, 3573. Bryan, J. C.; Geib, S. J.; Rheingold, A. L.; Mayer, J. M. *J. Am. Chem. Soc.* **1987**, *109*, 2826.
(9) CpRu(PPh$_3$)$_2$OTf: ^{1}H NMR (C$_6$D$_6$) δ 4.34 (5 H, s), 6.9–7.3 (30 H, m); ^{31}P{H^1} NMR (C$_6$D$_6$/toluene) 46.43 ppm. Anal. Calcd for C$_{42}$H$_{35}$F$_3$O$_3$P$_2$RuS: C, 60.07; H, 4.17. Found: C, 60.75; H, 4.54.
(10) The use of triflate salts has had a major impact on the synthetic chemistry of the ruthenium and osmium pentaammines, see: Lawrance, G. A. *Chem. Rev.* **1986**, *86*, 17.

0002-7863/88/1510-2332$01.50/0